

Oscillations, Cessations, and Circulation Reversals of Granular Convection in a Densely Filled Rotating Container

Frank Rietz and Ralf Stannarius

Otto-von-Guericke-University, D-39106 Magdeburg, Germany

(Received 13 December 2010; published 16 March 2012)

We study spontaneously forming convection in a container that is almost completely filled with a bidisperse granular mixture. The container with an aspect ratio close to 1 rotates slowly about a horizontal axis. In this geometry, single vortex rolls are observed in the cell plane, after a spontaneous symmetry breaking. The circulation of grains produces nonuniform segregation patterns of the mixture that in turn interact with the convective flow. We describe oscillatory modulations of the convection velocity, cessations and spontaneous reversals of the circulation. All these features are absent in multiroll granular convection.

DOI: 10.1103/PhysRevLett.108.118001

PACS numbers: 45.70.Mg, 45.70.Qj, 05.65.+b, 47.54.-r

Granular matter is well known to exhibit numerous counterintuitive effects when it is agitated, for example, the spontaneous segregation of mixtures [1], the formation of local dynamical structures such as oscillons [2] and sand dunes [3], or convection patterns [4]. A classical type of experiment is that of horizontal, rotating containers filled with granular mixtures. The majority of these experiments deal with rotating drums that are approximately half full. There, fluidization of the granulate surface plays the most important role in the emergence of axial segregation patterns. There are a few experiments [5–8] and simulations [9] that deal with almost completely filled horizontally rotated drums. Contrary to expectation, these studies demonstrate that pattern formation can even occur when fluidization is strongly inhibited. Granulate in an almost full container produces circulation patterns when the container is rotated slowly [5,6].

A particularly interesting geometry is the small aspect ratio of a nearly square-shaped flat cell. There, single rolls with unconventional properties can be observed, which form as a result of spontaneous symmetry breaking. They show more complex behavior than roll arrays [5,6], and differ from other known types of convection rolls in granular media [6]. We demonstrate that in our special geometry a complex interaction of segregation and convection patterns can lead to oscillatory dynamics that was so far not observed in comparable experiments. As known, e.g., from geophysical systems, the combination of circulation and segregation can have considerable consequences [10].

Single roll convection has been extensively studied in Rayleigh-Bénard convection under very high Rayleigh numbers in cylindrical [11] or (quasi-) two-dimensional rectangular containers [12] of aspect ratio 1. Single large scale convection rolls perform diffusive azimuthal motion and occasional flow reversal after cessation of the vortex flow. Irrespective of the very different materials and driving mechanisms, there are some formal similarities to our granular convection rolls, for example, the “grainy”

structure of vortices (as opposed to laminar fluid flow), the existence of boundary layers at the top and bottom plates, and the strong local density fluctuations in the convecting material.

We fill flat transparent boxes of $60 \text{ mm} \times 80 \text{ mm}$, $80 \text{ mm} \times 80 \text{ mm}$, and $83 \text{ mm} \times 110 \text{ mm}$ (width $x \times$ height y) with fixed depth $z = 5 \text{ mm}$ [Fig. 1(a)]. The aspect ratios $x:y$ are thus 0.75 and 1.0, resp. A row of boxes is assembled into a bigger container [Fig. 1(b)] so that multiple experiments can be recorded simultaneously. The granular material is a 50%:50% (by volume) bimodal size mixture of sieved $300 \pm 50 \mu\text{m}$ and $900 \pm 100 \mu\text{m}$

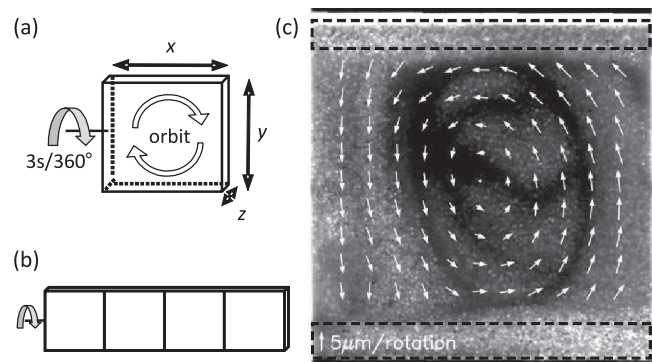


FIG. 1. (a) Sketch of the experimental setup. Arrows indicate the sense of the container rotation and one of two possible directions of the granulate orbit. (b) Sketch of the container array for simultaneous experiments. (c) Segregation pattern after 107 000 rotations. The transmission intensity reflects the local composition of the mixture (see text). Dashes mark the borders of fluidized regions at the container’s bottom and top edges. The white stripe on top is the free volume ($\approx 2\%$) above the granulate (overexposure in the contrast enhanced image makes the cell appear less filled). The overlaid vector field indicates the collective grain motion. In this sample, a full orbit takes $\approx 40\,000$ rotations (average angular velocity $\omega = 1.6 \times 10^{-4}$ /rotation, $x = y = 8 \text{ cm}$, fill level $C = 0.638$).

glass beads (Glasstrahlwerk Würth, type MGL) with density $\rho = 2.50 \text{ g/cm}^3$.

The boxes rotate about their central horizontal axis at 20 rpm. Inertial effects are negligible, the Froude number is below 0.02. Every 20 rotations, the box is gradually slowed down and stopped. A camera takes a picture of the box in vertical orientation, in transmitted light. As the pattern and flow on the front and back sides are essentially identical, only one side of the cell is captured with the camera. We record images for periods of 15 000 to 360 000 rotations (2 weeks).

The cell filling fraction is a crucial parameter for the experiment. The height of the granular bed is not a reliable measure because it is influenced by unavoidable segregation and compaction during filling [13] and in the course of the experiment. A reproducible measure for the fill state is $C = m/(\rho V_{\text{total}})$. V_{total} is the total container volume and m is the mass of the glass beads. Without any further compacting by shaking after filling, a maximum fill ratio of $C \approx 0.65$ can be achieved. Convection rolls emerge only when $C \geq 0.62$, i.e., for almost complete filling. The main part of the granular bed performs a collective circulating motion [Fig. 1(c)]. After a few hundred rotations, a ring-shaped segregation pattern is visible in the central part of the rotating box. Dark (bright) areas indicate regions enriched with small (large) bead species. The local net flow does not balance to zero. Instead, we find stable orbits, indicated by arrows in Figs. 1(a) and 1(c). We use the term “orbit” to describe the grain convection, in order to avoid confusion with the rotation of the box. The granulate orbits about the z axis, perpendicular to the container rotation axis x [Fig. 1(a)]. In the course of the experiment, the orbit’s center can shift in the cell. Fluidization, i.e., individual grain motion, is limited to narrow zones at the cell top and bottom, alternating at each half rotation of the cell [dashed zones in Fig. 1(c)]. These zones drive the convection (see below).

In some boxes with aspect ratio 1, convection sets in with two counterpropagating rolls, and we observe transitions from single rolls to two rolls and vice versa. The preferential spatial periodicity of the convection pattern is obviously slightly smaller than 2 times the cell height. In quadratic cells, roll pairs may compete with single rolls. When the aspect ratio is 0.75, only single rolls remain.

We derive mean displacements of the beads from consecutive images by calculating cross-correlations in $9 \text{ mm} \times 9 \text{ mm}$ segments [Fig. 1(c)]. The fast individual grain motion in the fluidized zones cannot be quantified with our method, these zones are therefore not included in the computation of the flow field.

As a reasonable approximation, we will treat in the following the flow field as a simple rotation, quantitatively described by the angular velocity ω . The curl of the in-plane velocity field \vec{v} is related to ω by $\|\nabla \times \vec{v}\| = 2\omega$. For data evaluation we employ Stokes’ theorem and

approximate the curl for each grid cell by the velocity integral along the surrounding grid points [14]. In order to reduce the effect of outliers in image processing, we take the median of all local ω to characterize the global flow. Positive ω corresponds to counterclockwise flow in our reference system (clockwise when viewed from the reverse side of the cell).

Circulation usually starts clockwise or counterclockwise that can change spontaneously on long time scales. Statistically, the circulation sense is preserved for an order of 10^4 rotations. Figure 2 shows the long-term dynamics of a few typical runs (time in units of cell rotations). One finds stable orbits in one direction, random flow reversals, cessations of the convection, and regular oscillations of the flow, with or without reversal of the circulation. In Fig. 2(b), flow ceases for an extended period but starts again after 320 000 rotations (not shown). In all experiments, we find a maximum $|\omega|$ of the order of 10^{-3} /rotation.

The height of the granular bed varies with the nonstationary segregation process (height differences $< 0.5 \text{ mm}$). There is no systematical relation between height and convection velocity. Also, the air humidity protocol (15%–30% rel. humidity for Fig. 2) shows no correlations with the observed dynamics.

Cells with multiple convection rolls [5,6] do neither show comparable oscillations nor flow reversal, convection is stationary. A continuous material exchange between neighboring rolls in an array or pair (e.g. Fig. 1 in Ref. [5]) can suppress the fluctuations.

Asymmetries in the initial preparation of the cells (e.g., partial demixing during filling) might preselect the initial

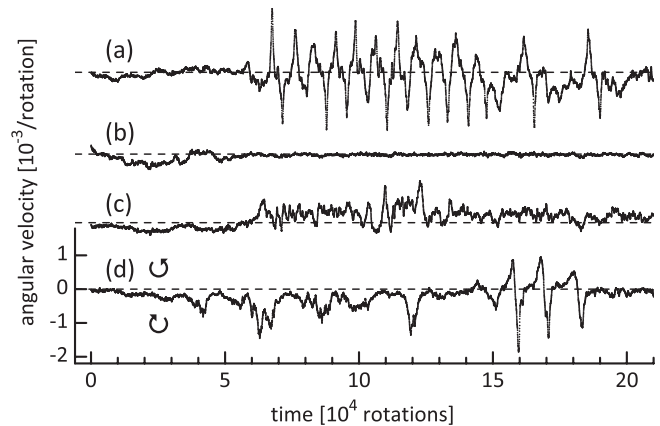


FIG. 2. Typical measurement of the average vortex flow velocity with regular circulation, fluctuations, reversals of the vortex sense, cessations and oscillations in four simultaneous experiments. Curves (a)–(c) are shifted vertically for clarity, dashes mark their baselines. The curved arrows above and below the dashed line indicate the sense of the circulating orbit [white arrows in Fig. 1(a)]. ($x \times y = 6 \text{ cm} \times 8 \text{ cm}$, $C = 0.640$). Each data point in Figs. 2–4 is averaged over 200 rotations.

sense of convection flow. In order to avoid this, we have developed a special axially symmetric preparation technique [6]. We start with two stratified, completely demixed grain layers (analogous to Fig. 5 in [6]). These layers mix completely within a few hundred rotations. After that, the convection starts in a random sense. Also, the general dynamics is insensitive to axial asymmetries of the container, e.g., if one vertical side of the boxes is covered with sandpaper (with granularity of the small bead size). Such a modification does not lead to a preference of one circulation sense. The sense of the orbit is also insensitive to an inclination of the cell rotation axis. All this is expected since front and rear sides interchange with each half turn of the cell.

The cessation and occasional spontaneous reversal of convective flow is remarkable, but not unique to this experiment. As stated above, these effects have been described in thermally driven convection experiments at high Rayleigh numbers [11,12]. Our quasi-2D system does not allow azimuthal fluctuations, it is expected to (and it does) behave more like flow in a cuboid geometry [12] rather than in a cylinder [11].

In addition to spontaneous flow reversals, the self-organized segregation can lead to regular oscillations. In Fig. 3(a) the angular velocity ω of such an oscillating roll is shown as a function of cell rotations. It is more instructive to plot the same data as a function of the number of orbits $\frac{1}{2\pi} \int \omega dt$ of the granulate [Fig. 3(b)]. The flow changes from fast to slow and back with a period of roughly half an orbit. The experiment in Fig. 3(a) is an example where the global direction of the convection changes its sign spontaneously (the simultaneous onset of oscillations is a coincidence). Details of oscillations vary between different experiments.

Another run is shown in Fig. 3(c). After 2.5 clockwise orbits the flow passes over to an oscillatory regime. The direction reverses repeatedly, which is reflected as loops in the figure. Roughly 0.15 counterclockwise orbits are followed by approximately 0.65 clockwise orbits, resulting in a net half orbit in clockwise direction during one oscillation. Even though in this cell the sense of orbital motion changes, the overall convective flow is faster than in the nonoscillating regime [inset in Fig. 3(c)]. Oscillations seem to increase the efficiency of the particle transport, as compared to nonoscillating flows.

In the experiment presented in Fig. 4(a), the oscillations were recorded over 200 000 rotations (8.5 days). After a short transient (≈ 2 orbits) one can identify a half orbit period. This modulation is overlaid by a period of one orbit. A sequence of peaks (marked by letters A to D) approximately repeats during every orbit.

The observed periodicity of the convection suggests that the flow modulation is related to the particular segregation structure. The influence of the local segregation was checked by averaging images at each of the 4 stages

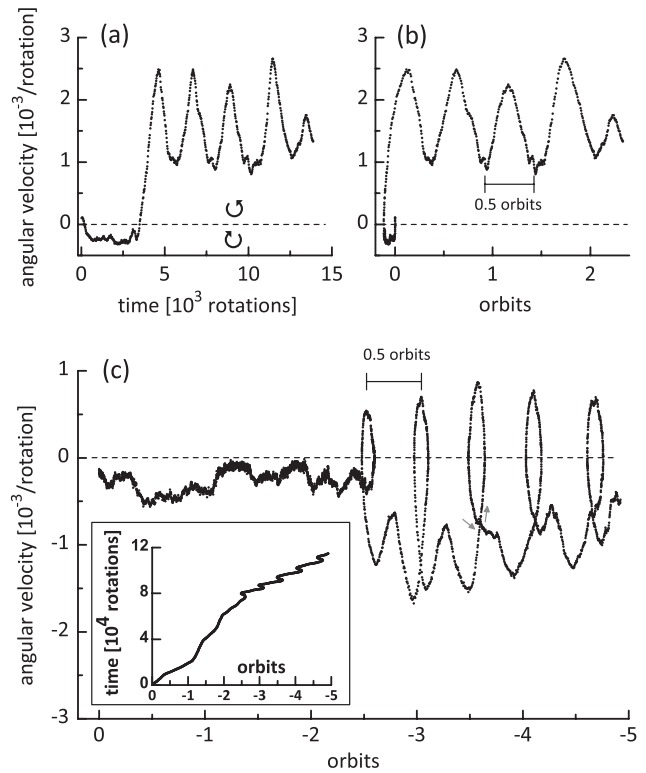


FIG. 3. (a) Angular velocity as a function of time and (b) for the same experiment as a function of the number of orbits. After a slow clockwise motion the direction reverses and the flow amplitude increases. The flow now circulates with a period of a half orbit. ($x \times y = 8.3 \text{ cm} \times 11 \text{ cm}$, $C \approx 0.63$). (c) After fluctuating around a low amplitude the flow in this experiment evolves into an oscillating regime with higher peak velocities that are combined with direction changes (“loops”). The inset shows the time needed for the orbits. ($x = y = 8 \text{ cm}$, $C = 0.638$).

A–D in Fig. 4(a), to extract typical features of the segregation states [Fig. 4(b)]. Similar patterns are found for the experiments in Fig. 3. The distinct arrangements of the zones enriched with small particles (dark areas) are marked with crosses at four different container positions. The segregation spots orbit with approximately the same velocity as the particle clusters. Beads from the convecting central region can enter the more loosely packed fluidized zones, and the net flow is balanced by reentrance of particles towards the central cell area. During transport along the fluidized edges, small beads are ‘sieved out’, which creates and maintains the segregation. We conclude that the periodicity of the flow amplitude relates to the position of the small particle enriched clusters in the partially demixed regions during orbiting. Figure 4(b) demonstrates that the convection is faster when the small particle enriched regions move out of a fluidized surface zone (states A,C), whereas the velocity is slower when such regions are driven into a fluidized surface zone (states B,D). Because of the top-bottom symmetry of the cell, one should expect

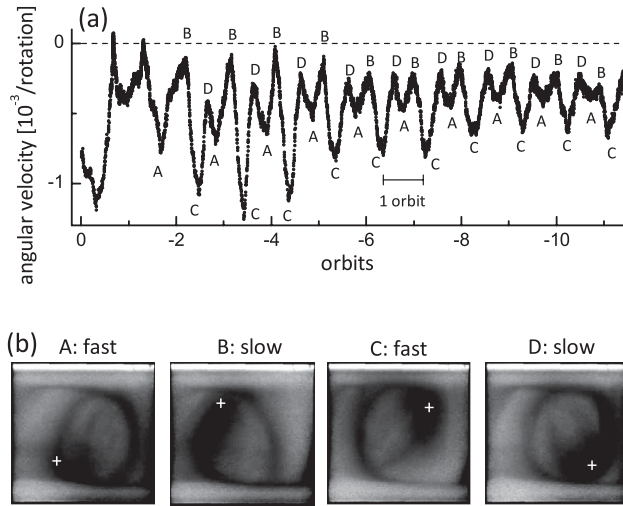


FIG. 4. (a) Angular velocity as a function of the number of orbits. The flow oscillates with a periodicity of half an orbit and shows a superimposed four-fold periodicity (peaks labeled A–D). ($x = y = 8$ cm, $C = 0.650$) (b) Averaged flow patterns in four phases of the cycle reveal the circulation of the nonuniform segregation cluster (+), clockwise flow.

pairwise similar velocities for states A,C and states B,D, respectively. Differences between states A and C on one hand and states B and D on the other hand can thus be related to a direct interaction of the segregation pattern and local granulate composition with the convection stream.

It is obvious that a homogeneously mixed state would be an unstable situation. Thus almost all experiments developed clusters enriched with small and large particles, respectively. Whether the oscillation is periodic or not depends on the spatial distribution and stability of these clusters. In some cases, the granulate develops two opposing clusters enriched with small beads on the orbit. Convection works also with grains that have a size distribution of a certain width to avoid crystallization. Strictly monodisperse grains tend to crystallize, which inhibits convection [5,6].

Figure 4(b) suggests that the fluidized zones play a significant role in the convection process. Therefore, it is appropriate to analyze the individual particle dynamics in different parts of the cell. For a semiquantitative representation of the local fluidization state, we visualize the temporal fluctuations between consecutive images (Fig. 5). We depict the absolute differences of brightness, normalized by the local intensity. Bright (yellow) and dark (blue) areas in this figure symbolize regions of large and small fluctuations of the particle arrangements, i.e., fast and slow grain displacements, respectively. As seen in the figure, the top and bottom zones of the granulate in the rotating cell contain highly mobile particles. We mention in passing that these zones rotate in the same sense as the cell, with velocities of the order of several hundred micrometer per rotation [6]. The rotation sense is similar to the bulk motion

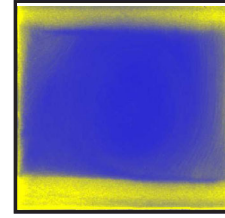


FIG. 5 (color online). Fluctuations of the particles (see text) averaged over all images taken during the last orbit of Fig. 4(a), brightness or color indicates the strength of fluctuations. Highly fluidized zones (bright, yellow) are observed at the top and bottom, but smaller zones also appear at left- and right-hand sides.

in half filled cylindrical tumblers. The height of these fluidized layers is 5 to 6 mm each, of the same order as the cell thickness z , but decreases with decreasing free volume above the granulate. Granulate in the convective bulk is partly transported into the fluidized zones and their material composition varies. This is the fundamental process responsible for oscillations of the convection velocity [6]. Different segregation patterns in the fluidized regions are seen in states B and C in Fig. 4(b). Because of the higher mobilization in the fluidized regions, the particles are redistributed and the small species is sieved out while moving along the horizontal with the convection flow. In the experiments shown in Figs. 3(c) and 4, additional narrow fluidized layers at the left and right sides of the cell (see Fig. 5) are observable. These lateral zones are not developed in all cells.

In contrast to rotated containers, there is a large variety of convection scenarios in strongly vibrated granular systems. Single rolls in simulations of shaken systems have been explained by gradients in granular temperature [15], or they appear at special driving conditions [16]. They are found also in a few experiments [4]. These are connected to Faraday heaping. This effect vanishes at reduced air pressure [17] and when the acceleration is less than 1.2 times the gravity. As opposed to the Faraday instability, our system is not influenced by air [6] and the effective acceleration (during sliding of the grains) is lower than g .

From the experiments, we draw the following conclusions on the segregation, convection, flow reversal and oscillation mechanisms: Since the stratified preparations led to a mixing of the granulate first, we consider that an initial segregation is not responsible for the onset of convection. Rather, the subsequent segregation in the vortex center accompanies the convective motion. This segregation is not uniform: at long time scales the granulate often develops one or two clusters that orbit the vortex center. During this orbiting motion, the position of these clusters relative to the fluidized layers modulates the convection velocity.

We thank Thomas John for technical assistance and James R. Third for critical remarks to the manuscript.

- [1] Y. Oyama, *Sci. Pap. Inst. Phys. Chem. Res. (Jpn.)* **6**, 600 (1939).
- [2] P. B. Umbanhowar, F. Melo, and H. L. Swinney, *Nature (London)* **382**, 793 (1996).
- [3] See, e.g., I. Livingstone, G. F. S. Wiggs, and C. M. Weaver, *Earth Sci. Rev.* **80**, 239 (2007).
- [4] See, e.g., P. Evesque and J. Rajchenbach, *Phys. Rev. Lett.* **62**, 44 (1989); M. A. Naylor, M. R. Swift, and P. J. King, *Phys. Rev. E* **68**, 012301 (2003); R. J. Milburn *et al.*, *Phys. Rev. E* **71**, 011308 (2005); P. J. King *et al.*, *Eur. Phys. J. E* **22**, 219 (2007); R. M. Lueptow, A. Akonur, and T. Shinbrot, *Exp. Fluids* **28**, 183 (2000).
- [5] F. Rietz and R. Stannarius, *Phys. Rev. Lett.* **100**, 078002 (2008).
- [6] F. Rietz and R. Stannarius, *New J. Phys.* **14**, 015001 (2012).
- [7] H. P. Kuo, P. Y. Shih, and R. C. Hsu, *AIChE J.* **52**, 2422 (2006).
- [8] S. Inagaki and K. Yoshikawa, *Phys. Rev. Lett.* **105**, 118001 (2010).
- [9] A. Awazu, *Phys. Rev. Lett.* **84**, 4585 (2000).
- [10] J. M. N. T. Gray and B. P. Kokelaar, *J. Fluid Mech.* **652**, 105 (2010).
- [11] E. Brown and G. Ahlers, *J. Fluid Mech.* **568**, 351 (2006); H.-D. Xi, Q. Zhou, and K.-Q. Xia, *Phys. Rev. E* **73**, 056312 (2006); H.-D. Xi *et al.*, *Phys. Rev. Lett.* **102**, 044503 (2009).
- [12] K. Sugiyama *et al.*, *Phys. Rev. Lett.* **105**, 034503 (2010); A. Yu. Vasil'ev and P. G. Frick, *JETP Lett.* **93**, 330 (2011).
- [13] H. A. Makse *et al.*, *Nature (London)* **386**, 379 (1997).
- [14] C. C. Landreth and R. J. Adrian, *Exp. Fluids* **9**, 74 (1990); M. Raffel *et al.*, *Particle Image Velocimetry* (Springer, New York, 2007), Chap. 6.4.
- [15] R. Ramírez, D. Risso, and P. Cordero, *Phys. Rev. Lett.* **85**, 1230 (2000); D. Paolotti *et al.*, *Phys. Rev. E* **69**, 061304 (2004).
- [16] P. Sunthar and V. Kumaran, *Phys. Rev. E* **64**, 041303 (2001).
- [17] R. P. Behringer *et al.*, *Granular Matter* **4**, 9 (2002).